X-RAY DIFFRACTION STUDIES OF THE CRYSTALLINE STRUCTURE OF THE AVIAN EGG SHELL

C. J. CAIN *and* A. N. J. HEYN

From the Department of Physics, Auburn University, Auburn, Alabama. Dr. Heyn's present address is the Department of Biology, Louisiana State University, New Orleans

ABSTRACT From x-ray studies, it is concluded that the avian egg shell is composed of calcium carbonate in the calcite modification. In the main portion (crystalline layer) the calcite occurs in large crystalline areas oriented with the hexagonal axis (17.6 A) inclined at 28 to 16° from the normal of the shell surface. With respect to the other areas, orientation is present over limited areas. The mammilla layer contains crystallites in entirely random orientation.

The findings agree with the electron microscope observations by the second author (Heyn, 1936 *a* and *b*) according to whom large oriented crystals, spherulites, or dendrites would compose the main layer and small unoriented crystals the mammilla layer.

INTRODUCTION

The avian egg shell consists of about 94 per cent calcium carbonate, some organic matter, ovokeratin, and small quantities of magnesium carbonate. Light microscope studies have shown that three layers may be distinguished in the shell: the main layer, termed crystalline or spongy layer; the inner layer or mammilla layer, which consists of microscopic protruding knobs; and the outer layer or cuticle, which contains a large portion of the organic matter. (Stewart, 1935, and Young, 1951.) Electron microscope studies have been recently carried out by the second author (Heyn, 1963). The few x-ray observations made in the past have shown that the calcium carbonate occurs in the crystalline modification of calcite, and not in the aragonite form. (Foulkes *et al.*, 1958, and Mayneord, 1927.) These findings are in agreement with optical crystallographic observations by Stewart (1935) and Young (1951).

In the present paper a more detailed x-ray study of the crystallographic structure of the shell is presented. Not only photographic but also x-ray diffractometer techniques were used in which the orientation and size of the crystallites were determined.

The material studied consisted mainly of chicken egg shell. A few shells of other birds were studied for comparison.

I. DIFFRACTOMETER STUDIES OF THE INTACT AND GROUND SHELL

Experimental Procedure

For the diffractometer work the standard norelco diffractometer (Philips) was used. Both the intact shell and powdered shell material was studied. The presence of organic matrix did not affect the diagrams; previous dissolving of the matrix by boiling in weak potassium hydroxide or sodium sulfide solutions, to remove the organic material, had no effect on the x-ray diagram. The organic material was therefore not removed in the following experiments. The loose organic membranes on the inside of the shell, however, were always mechanically removed.

The "intact" samples were prepared by pressing a piece of egg shell on a flat support maintaining the original orientation of the shell as well as possible. The powdered material was spread in a thin layer on the support. The traces were obtained by glancing angle reflection from the respective surfaces, and each trace is a plot of the diffracted beam intensity *versus* the Bragg angle, copper $K_{\alpha_1\alpha_2}$ radiation being used.

Results

Fig. 1 shows the diffractometer traces from: finely *powdered* calcite (*a*), powdered egg shell material (*b*), and the interior (*c*) and exterior (*d*) surfaces of the *intact* shell. The locations and intensities of the peaks in both traces *a* and *b* are indentical and correspond to the ASTM data for calcite.

The pattern from the *interior* surface *c* of the intact shell is seen to correspond also to that of the ground shell shown in *a,* but the pattern from the *outer* shell surface *d* differs with regard to absence of and relative intensities of certain reflections. The (110), (113), and (202) peaks, for example, which arise from planes having interplanar spacings of 2.51, 2.30, and 2.10 A, respectively, are not present in the pattern of the outer surface of the egg shell. No change in the pattern of the outer surface was produced by a rotation of the intact sample through 90° in its own plane, demonstrating that the absence of these peaks cannot be ascribed to accidental registration of the discontinuities in the Debye-Scherrer rings resulting from oversized crystallites (see below).

Since the patterns from the two sides differ, it must be concluded that the reflected beam originates in each case from only a thin layer of the inside and outside surface of the shell; otherwise, identical patterns should have been obtained. This difference between the inner and outer portions of the shell can be explained by a difference in orientation of the crystallites in this portion. The inside layer must have random orientation, since the pattern corresponds to that of the powered material. The outside layer must have preferred orientation.

This conclusion was confirmed by the finding that after 100 microns of the inner

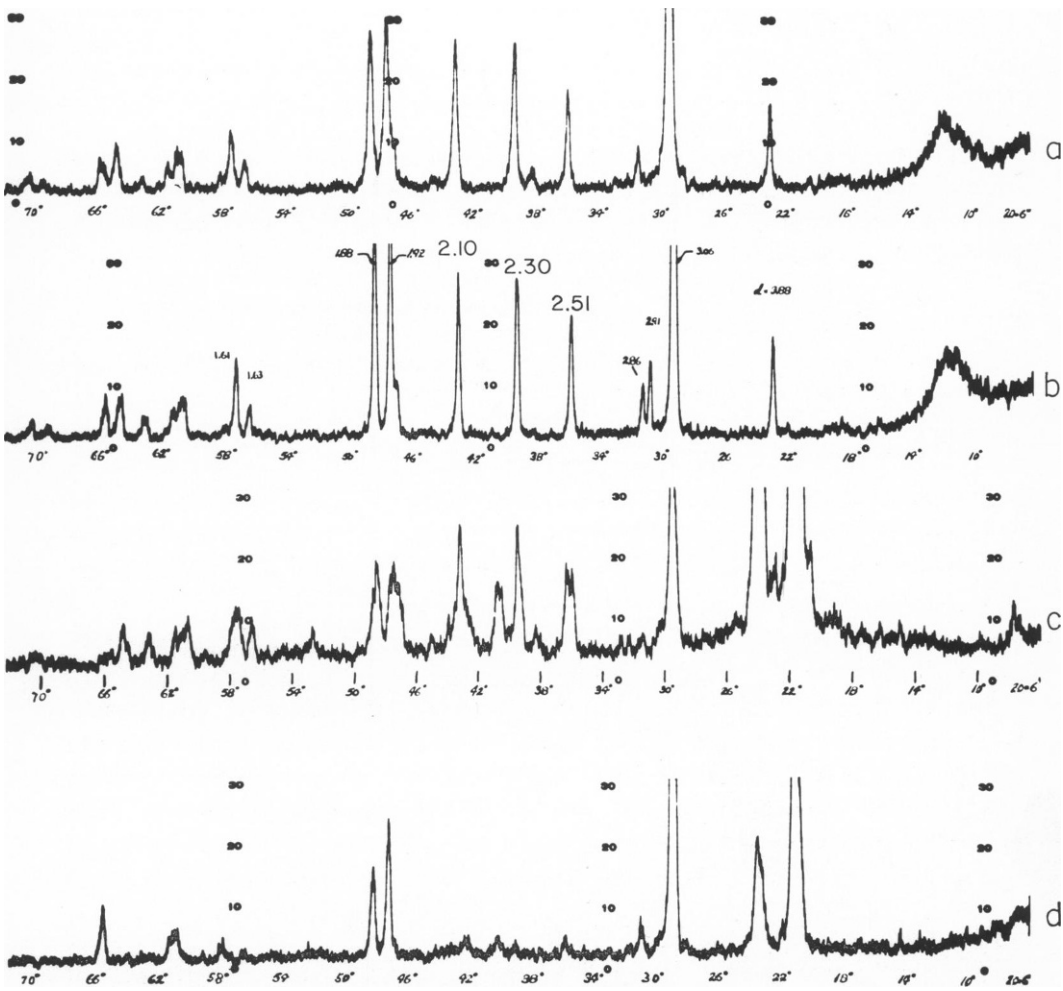

FIGURE 1 Diffractometer traces from: (*a*) powdered egg shell, ground 300 mesh; (*b*) powdered calcite, ground 300 mesh; (*c*) interior surface of the intact chicken egg shell, not ground; (*d*) exterior surface of the intact chicken egg shell, not ground.

shell surface had been removed by grinding, the x-ray diffraction pattern obtained by glancing angle diffraction from the remaining underlying inside surface was identical with that of the outside surface, missing the same reflections as the latter one. It can be concluded therefore, that the inner stratum consists of a layer of randomly oriented calcite crystals, whereas the remaining part of the shell must have preferred orientation. Before further study of the preferred orientation, the crystallite size will be considered.

II. CRYSTALLITE SIZE AND ASTERISM

The diagram of the egg shell shows typical asterism. Around the primary beam radial streaks are observed, illustrated in Fig. 3. This phenomenon may be ascribed to the presence of large crystallites and/or to lattice distortion. Besides asterism, the diagram shows diffraction rings containing separate diffraction spots instead of hav-

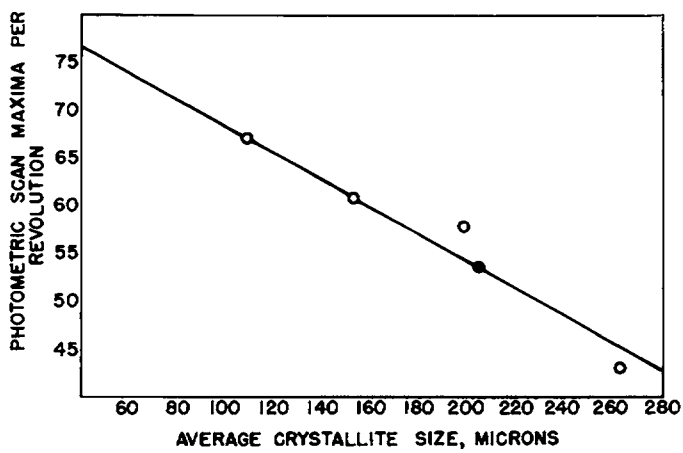

FIGURE 2 Calibration curve for particle-size determination (○) by method described in text and crystallite-size determination (●) in egg shell.

ing a continuous appearance, Fig. 3. This points to the presence of large crystals or their equivalent, each spot originating from an individual crystallite or crystalline area. Since large crystallite size can explain both features simultaneously without reference to lattice distortion, it is possible that only this cause is underlying the phenomena observed. For this reason a detailed study of the crystallite size was made first.

Experimental Procedure

For a direct estimate of the crystallite size, a method similar to that of Aborn and Davidson (1929), was used in which the number of diffraction spots in the rings is used for determining the crystallite size. Transmission patterns were prepared from ground calcite of decreasing particle sizes. Calibration curves were prepared by plotting the number of

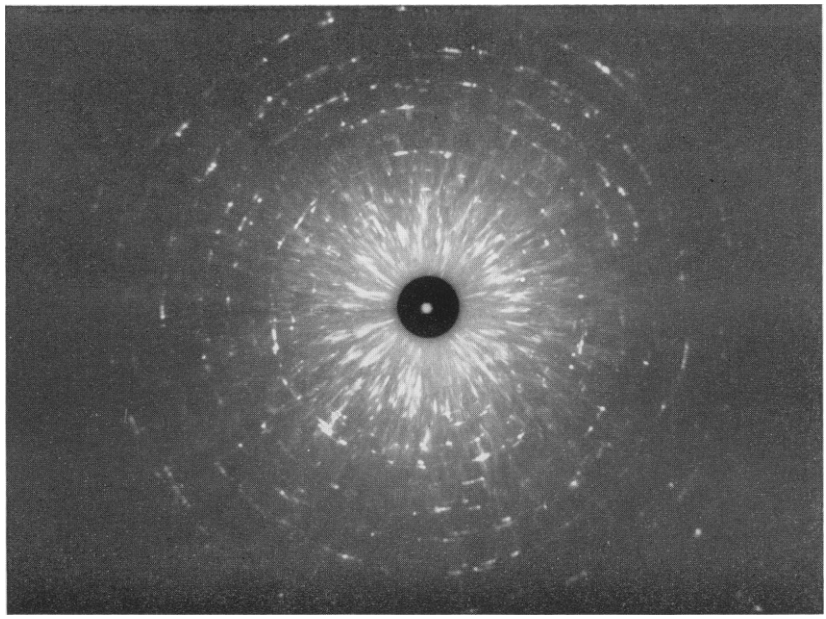

FIGURE 3 Typical diffraction pattern of the intact chicken egg shell showing asterism at low angles and discontinuous diffraction rings.

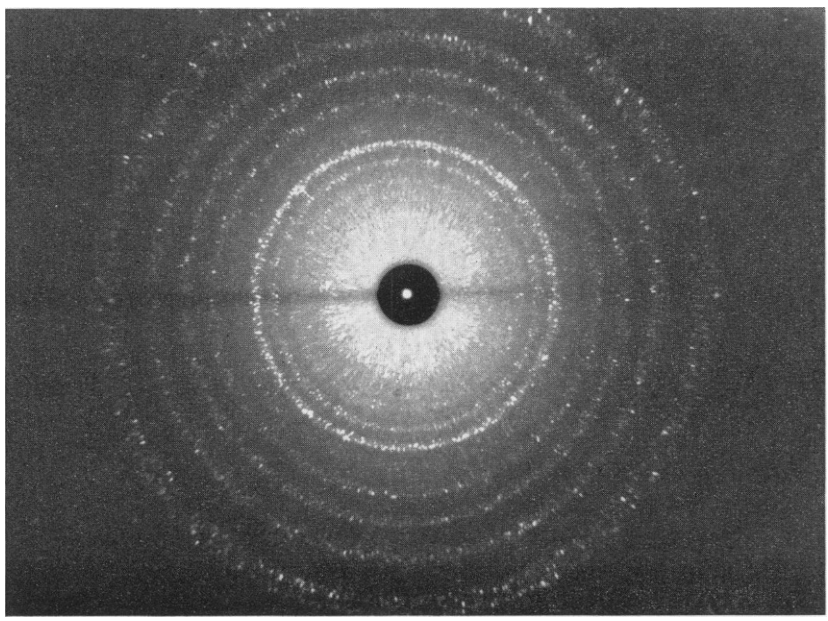

FIGURE 4 Diffraction pattern of the innermost crystallites of the chicken egg shell; the nearly continuous diffraction rings indicate small crystallite size.

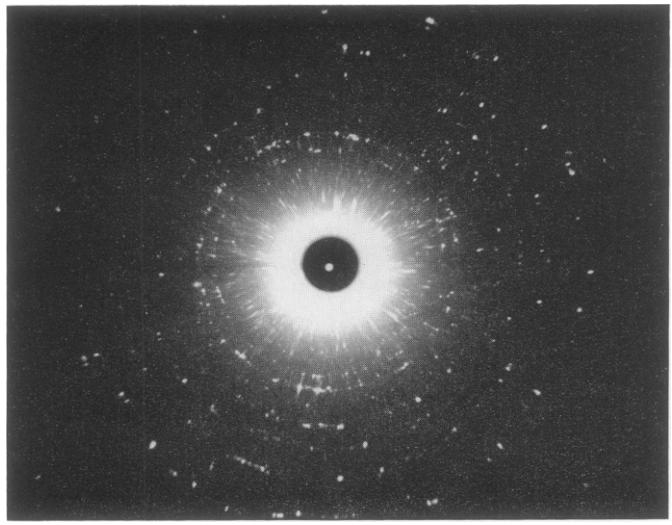

FIGURE 5 Diffraction pattern of the quail egg shell.

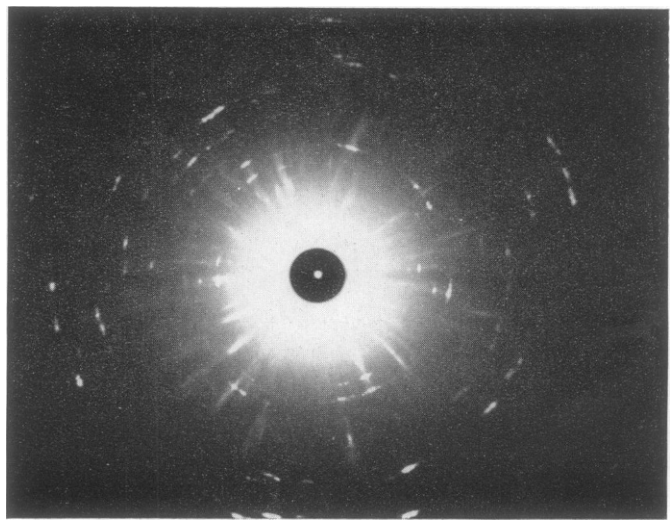

FIGURE 6 Diffraction pattern of the ostrich egg shell.

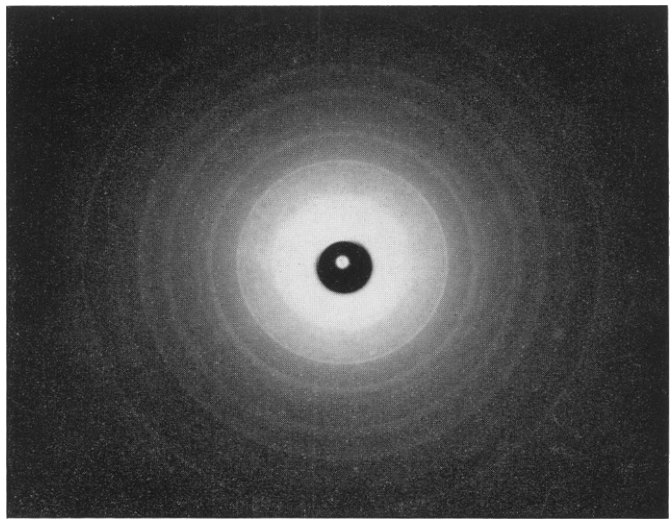

FIGURE 7 A typical pattern from pole-figure series described in text; beam-to-normal angle $\phi = 23°$ (series 1, see Table I).

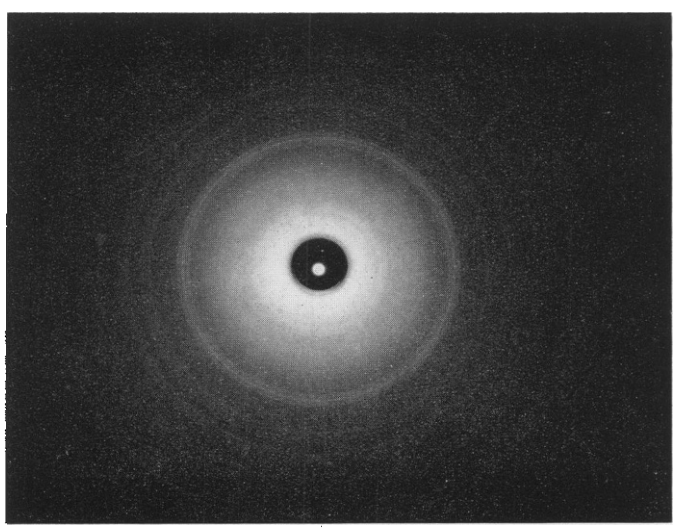

FIGURE 8 Same as Fig. 7; $\phi = 45°$.

diffraction spots *versus* particle size. The number of diffraction spots in the diffraction rings from the egg shell was compared with that in the calibration patterns and curve. This comparison was made by both visual estimation and instrumental measurement. In the latter case the patterns were scanned by means of a recording densitometer equipped with a rotating radial slit of 0.1 mm in width extending from the center in radial direction. With this instrument the discontinuities of the central streaks and of the spots in the diffraction rings were scanned simultaneously. A calibration curve was prepared in this case by plotting the number of discontinuities in density per revolution of the slit against the known crystallite sizes for each of the various standard patterns. The flat film x-ray pictures used were taken at a sample distance of 3 cm.

Results

With the method described above, the dimension of the crystallites (or their equivalent) in the egg shell was determined. Fig. 2 shows the calibration curve and the data from the egg-shell pattern. The number of diffraction spots in the diffraction ring from the egg shell corresponds to a particle size of 200 microns.

In order to explain the *asterism,* a diagram for ground calcite of a particle size corresponding to the one of the egg shell was prepared. A comparison of this diagram with the one of the egg shell showed the same degree of asterism. It may be concluded, therefore, that the asterism is sufficiently explained by the size of the crystallites or their equivalent, and that the assumption of lattice distortion is at least not required for its explanation.

A few shells from the eggs of different birds were also compared in the above way. It could be concluded by mere visual comparison of the diagrams that the interior surface layer of the chicken egg shell (Fig. 4) and the quail egg shell (Fig. 5) have a much smaller crystallite size, and that the ostrich egg shell (Fig. 6) has a much larger crystallite size than the main layer of the chicken egg shell.

III. CRYSTALLITE ORIENTATION

In order further to study the preferred orientation in the outer layer of the egg shell, a modified pole-figure technique was employed. The customary pole-figure method consists of the preparation of a series of diffraction patterns corresponding to different angles between the incident beam and the specimen surface, and the study of the variation of the diffraction pattern as a function of the angle. From this information it is possible to locate the poles (*i.e.* the normals to the crystal planes) upon a hypothetical reference sphere around the specimen. The pole figure is a two-dimensional representation of the locations of the poles on the reference sphere and provides a complete description of the crystallite orientations within the sample. If the usual methed is employed for the construction of the pole figure, it is essential that the diffraction rings or arcs be sufficiently smooth or continuous so that their intensities and angular extent may be determined. Because of the discontinuous nature of the diffraction rings in the egg-shell pattern it was necessary to alter the usual method.

Experimental Procedure

The procedure used in this study was similar to the customary technique in that x-ray patterns were obtained under various angles of the incident beam with the surface of the material. In contrast to the usual method, however, the film was rotated during exposure, the axis of rotation being collinear with the primary beam. The purpose was to spread the discontinuous Debye-Scherrer rings, which resulted from large crystallite size, into artificially smooth continuous rings similar to those of a normal powder pattern. It was thus possible to make a visual estimate of the relative intensities of these rings.

The sample used for this portion of the work was taken from a specimen of egg shell from which the inner layer of randomly oriented crystallites had been removed by careful grinding until the diffractometer patterns from the inner and outer surfaces agreed. In the preparation of the pole-figure patterns, the sample was first tilted through successive angles around an arbitrary axis lying in the plane of the shell (the "horizontal" axis). A second series of patterns was similarly prepared, the specimen being now tilted about a perpendicular axis in the plane of the shell (the "vertical" axis).

Following the above method, diffraction pictures were taken at angles of 0°, 9°, 23°, 32°, 45°, 54°, and 60° between the x-ray beam and the shell normal. The intensities of the Debye-Scherrer (110), (102), (202), and (116) rings were estimated visually and tabulated in Table I as a function of specimen orientation about each of the mutually perpendicular axes described above.

TABLE I

VISUALLY ESTIMATED INTENSITIES OF DIFFRACTION RINGS USED IN POLE-FIGURE DETERMINATION AS DESCRIBED IN TEXT

Film No.	Beam-to-normal angle (degrees)	Intensities Reflecting planes (102)	(202)	(110)	(116)
Series I (horizontal tilt axis)					
A	0	Medium	Strong	Absent	Very weak
D	9	Very weak	Medium	Very weak	Absent
B	23	Absent	Weak	Very weak	Medium
G	32	Absent	Absent	Medium	Medium
C	45	Medium	Absent	Absent	Very weak
F	54	Absent	Weak	Absent	Weak
Series II (vertical tilt axis)					
A1	0	Absent	Absent	Absent	Absent
B1	9	Absent	Medium	Weak	Absent
C1	23	Absent	Absent	Absent	Very weak
D1	32	Medium	Absent	Absent	Very weak
E1	45	Medium	Absent	Weak	Medium
F1	54	Absent	Absent	Absent	Absent
G1	68	Absent	Absent	Absent	Absent

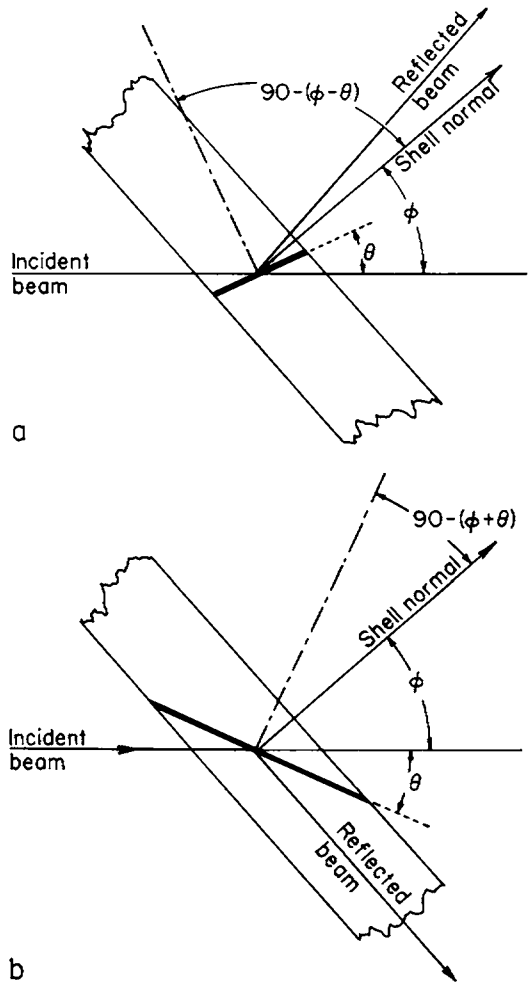
90-(ϕ-θ)
Reflected beam
Shell normal
ϕ
θ
Incident beam
a
90-(ϕ+θ)
Shell normal
ϕ
Incident beam
θ
Reflected beam
b

Results

Marked differences were found in the relative intensities of the diffraction rings as a function of specimen orientation with respect to the beam direction, Figs. 7 and 8 illustrate this briefly. This variation of the Debye-Scherrer rings conclusively established the presence of preferred orientation in the specimen. The data in Table I moreover allowed the quantitative calculation of the angular position of the crystal planes in the shell and of the directions of the poles, so that a rough pole figure could be constructed. It could be concluded that the hexagonal *c* axis (17.6 A) in the main layer of the shell must be inclined at $28 \mp 16°$ from the normal of the shell surface. Details are given in the following.

Calculation of Possible Pole Locations. It may be seen from Figs. 9*a* and 9*b* that if, after a rotation of the shell through an angle ϕ, a set of crystallographic planes fulfills the Bragg reflection condition by meeting the incident beam at the Bragg angle θ, the pole of this set of planes must lie either $(90° + \theta)$ or $(90° - \theta)$

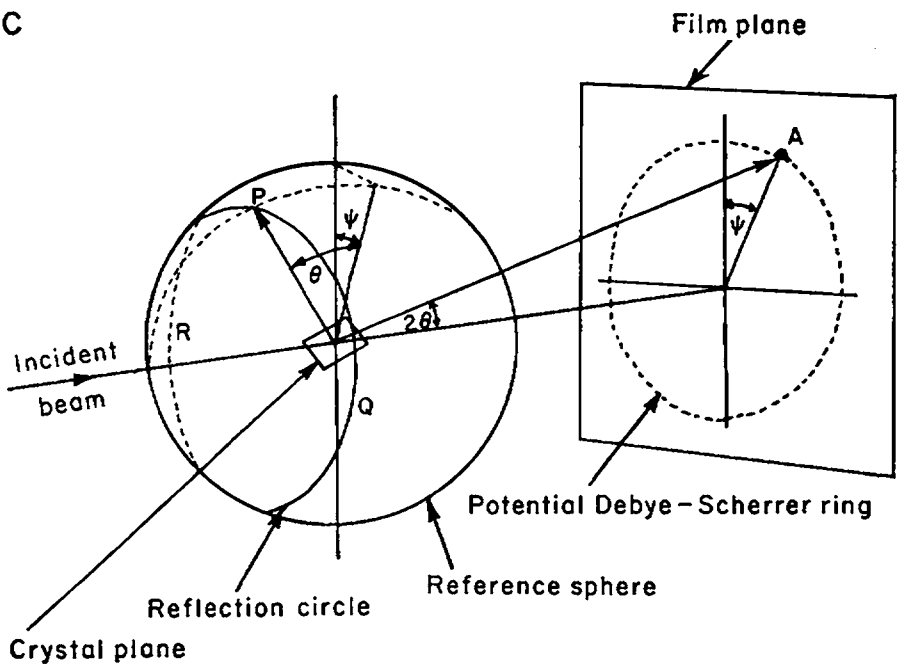

FIGURE 9*a* Cross-section of egg-shell sample showing a set of crystal planes reflecting at Bragg angle θ with respect to incident beam.

FIGURE 9*b* Alternate orientation of the same set of plans allowing Bragg reflection at the same specimen angle ϕ contributes to same diffraction ring as orientation shown in *a*.

FIGURE 9*c* Reflection geometry showing reference sphere surrounding a set of reflecting planes, the reflection circle *PQR*, and the pole *P* of the reflecting planes.

away from the primary beam. The choice of sign arises since the pole may have been moved onto either end of a given diameter of its reflection circle (see Fig. 9*c*) by the rotation of the sample through the angle ϕ, and the diffracted beam observed may be due to either of these possibilities. If the azimuthal coordinate of the resulting diffracted beam were known, the position of the pole on its reflection circle and consequently the orientation of the reflecting planes could be completely determined. But owing to the rotation of the film required in this method and the consequent artificial uniformity of the Debye-Scherrer rings, this azimuthal information is not available. The rotation of the specimen first around some vertical tilt axis, and next around an axis perpendicular to the first one, as described already under "procedure" above, was intended to compensate for this shortcoming.

Since each reflection was observed not simply for one value of the beam-to-normal angle ϕ but rather for a range of angles $\phi \pm \alpha$, the two possible reflection circles corresponding to each diffracted beam possessed a finite width and the angular zones $(90° + \theta \pm \alpha)$ and $(90° - \theta \pm \alpha)$ describe the possible locations of the pole relative to the incident beam when the Bragg condition is satisfied. These angular zones appear as latitudinal bands on the reference sphere, the bands being centered about the incident beam.

The rotation about one tilt axis thus yields one set of bands for the possible pole location (Fig. 10*a*). The rotation about the other tilt axis gives another set of bands (Fig. 10*b*). The pole studied must be located in the common areas of the two sets of bands (Fig. 10*c*).

As an actual example, the diffraction ring produced by the calcite (110) planes appeared with very low intensity when the shell normal was rotated through 9° or 23° about the *horizontal axis*, showed medium intensity when the shell's inclination was increased to 32°, and was absent at a shell inclination of 45° with respect to the incident beam. This reflection was thus recorded as produced by horizontal tilt angles of from 9° to 39°, half of the angular increment between successive patterns having been added at the upper limit of the range to take into account the fact that zero intensity must have been reached between 32° and 45°. Here ϕ is 24°, α is 15°, and since the Bragg angle θ for the calcite (110) reflection is 18° for copper radiation the possible orientations of the (110) pole consistent with this series of patterns are, relative to the incident beam, $(90° + 18° \pm 15°)$ and $(90° - 18° \pm 15°)$; *i.e.*, from 93° to 123° and from 57° to 87°. The corresponding pole locations on the reference sphere are shown stereographically in Fig. 11, in which both the shell normal and the horizontal tilt axis are in the plane of the paper and the angular zones described above are shown centered about the incident beam which is inclined at an angle ϕ (here 24°) with the shell normal. Only the upper hemisphere is depicted here for clarity.

When the specimen was rotated about the *vertical axis* the (110) reflection was observed at 9° and at 45°. To allow for the finite width of the reflections they were recorded as produced by vertical tilt angles of between 5° and 16° and between 39° and 50°. For the former reflection ϕ is 10½°, α is 5½°, and the possible pole locations are $(90° + 18° \pm 5½°)$; *i.e.*, between 102½° and between 66½° and 77½° from the incident beam. The corresponding pole locations on the reference sphere are shown stereographically in Fig. 11, the shell normal being in the plane of the paper and the bands describing the pole locations being centered around their respective incident beams. The vertical tilt axis is out of the paper at the center of the diagram.

The only (110) pole locations consistent with both the vertical and horizontal series

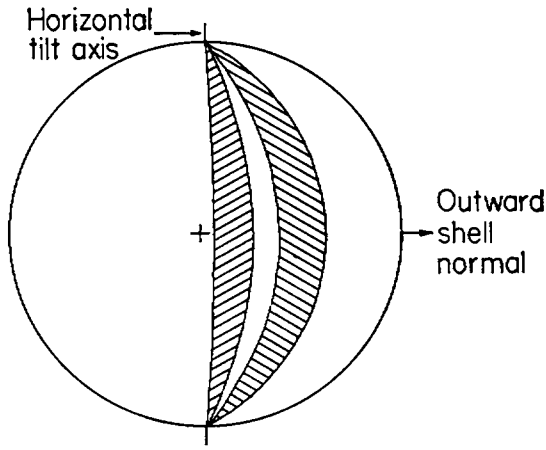

FIGURE 10*a* Angular ranges of possible pole locations. Vertical tilt axis prependicular to plane of paper.

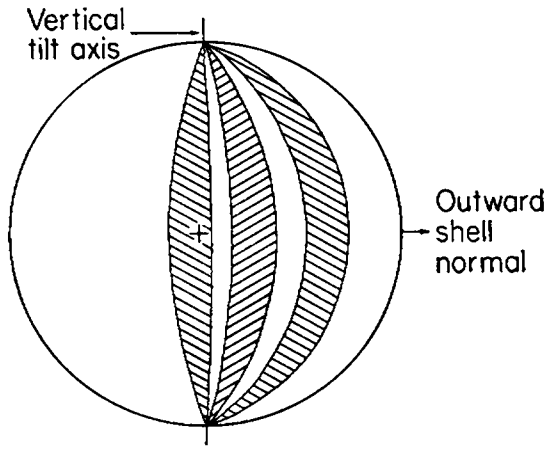

FIGURE 10*b* Angular ranges of possible pole locations. Horizontal tilt axis perpendicular to plane of paper.

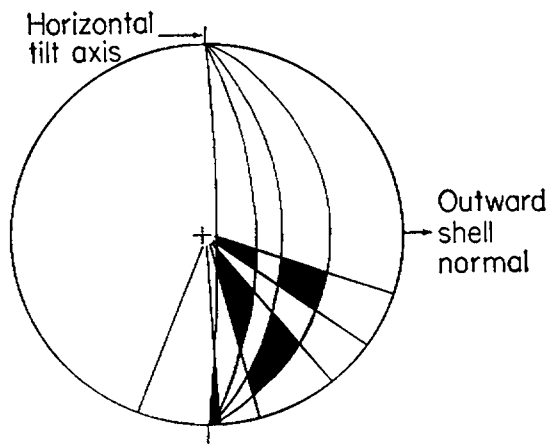

FIGURE 10*c* Possible locations of pole consistent with both series of pole-figure patterns. For clarity only one octant is shown; others are similar or reversed by symmetry.

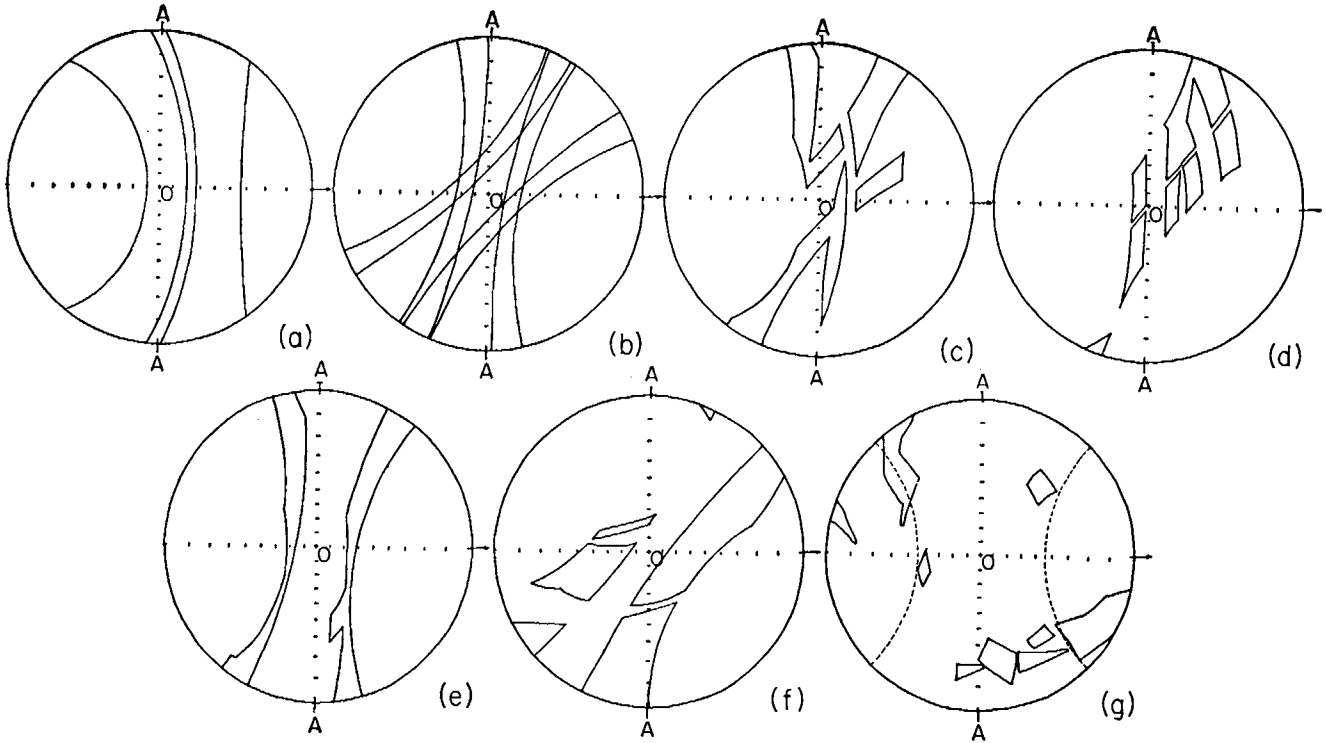

FIGURE 11*a* Stereographic projection showing possible locations of (110) pole on reference sphere as found from patterns of series I only. Arrow represents normal to outer surface of shell. Horizontal tilt axis *AA* is in plane of paper; vertical tilt axis is at center and out of paper at *O*.

FIGURE 11*b* Similar to Fig. 10: possible locations of (110) pole on reference sphere as found from patterns of series II only

FIGURE 11*c* Superposition of Figs. 11*a* and 11*b* showing all possible locations of (110) pole consistent with both series of diffraction patterns.

FIGURE 11*d* Possible locations of (102) pole.

FIGURE 11*e* Possible locations of (202) pole.

FIGURE 11*f* Possible locations of (116) pole.

FIGURE 11*g* Stereographic projection showing possible locations of calcite *c* axis on reference sphere as found by reference sphere model and curvilinear rulers (see text). Arrow represents normal to outer surface of shell. Locations appearing between dashed lines were rejected after comparison with diffractometer data.

of patterns consisted of those areas common to the two sets of "reflection bands" shown in Figs. 11*a* and 11*b*. These areas, defined by the intersection of the two sets of bands, are shown stereographically in Fig. 11*c* and represent the possible orientations of the (110) pole of the calcite crystals with respect to the shell normal (which is in the plane of the paper in the direction indicated).

In a similar fashion the possible locations of the (102), (202), and (116) poles were calculated. Rotation about the horizontal axis produced the (102) reflection within the angular ranges of between 0° and 9° and between 38½° and 49½° (including allowance for reflection width), while rotation about the vertical axis gave this reflection between 27½° and 49½°. The corresponding possible locations of the (102) pole on the reference sphere are shown stereographically in Fig. 11*d*. The locations of the (202) pole are shown in Fig. 11*e*, this reflection occurring from 0° to 27½° and from 49½° to 58½° (the upper limit of the latter reflection is uncertain and a reflection distributed symmetrically about 54° was assumed) for specimen rotations about the horizontal axis, and from 4½° to 16° for rotations about the vertical axis. Fig. 11*f* shows the possible locations of the (116) pole which caused reflections between 0° and 4½°, between 16° and 45°, and between 49½° and 58½° (here also a reflection symmetrical about 54° was assumed) for rotations about the horizontal axis, and between 23° and 49½° for rotations about the vertical axis.

In order to avoid the complications introduced by two-dimensional projections of spherical relationships, the possible locations of the poles to the four sets of reflecting planes in question were plotted on the surface of a large glass reference sphere. An arbitrary point on the sphere was selected to represent the pole of the outward-pointing normal to the egg shell. Within the equatorial plane defined by this pole two mutually perpendicular directions were chosen to represent the two tilt axes in relation to which the potential orientations of the various poles under study had already been deduced. The possible locations of the (102), (110), (202), and (116) poles were then plotted on the sphere in four respective colors, only the upper hemisphere being used since the lower hemisphere would contain the reflection of the same information.

Elimination of Pole Locations Inconsistent with Calcite Structure. Since it was necessary that all four poles fall simultaneously within their respective reflection zones on the reference sphere, certain combinations of pole locations on the sphere which were inconsistent with the interplanar angular relationships of the calcite crystal could be eliminated, since it would be impossible for the crystallites thus to satisfy the predicted pole configurations. In order to eliminate these impossible combinations, a curvilinear ruler was constructed from a plastic rod bent as required and shaped to conform to the curvature of the reference sphere. Five points marked on the ruler indicated the respective positions of the four relevant poles and of the crystallographic *c* axis of calcite. To include all possible pole configurations a second ruler was similarly constructed which was a mirror image of the first, representing the poles and *c* axis of a calcite crystal twinned with respect to that of the first ruler. By systematically sliding these curvilinear rulers over the surface of the reference sphere model and matching their markings with the potential pole locations on the sphere, the orientations of the crystallographic *c* axis which are shown stereographically in Fig. 11*g* were found to be those consistent with the actual calcite crystal structure. Here the *c* axis orientations shown are those obtained from data on the upper hemisphere only; similar reduction of data on the lower hemisphere would have resulted in an inversion of the same information.

As seen from Fig. 11*g*, a model of the egg shell in which the calcite *c* axis is parallel to the shell normal is not in agreement with the predictions of the two series of diffraction patterns, although such a crystallite orientation has been previously reported by observers using optical methods. The method employed here shows several possible orientations of the calcite *c* axis which may be roughly divided into two major groups: those orientations in which the *c* axis is inclined from 12° to 45° from the shell normal, and those orientations in which the inclination of the *c* axis is between 45° and 90°.

Incorporation of Diffractometer Information. Although the observed diffraction patterns of the two photographic series could be produced if the inclination of the *c* axis fell within either of the two angular zones described above, it was further necessary that any such orientation predicted by these patterns be consistent with the crystallite orientations implied by the absence of the (110), (113), and (202) peaks in the diffractometer plot of the egg-shell exterior surface (see Fig. 1*d*). In the normal use of the diffractometer, the specimen is placed within the instrument such that only planes of Miller indices (hkl) parallel to the surface of the specimen can contribute to the reflection peak. Hence the absence of the above three peaks in the diffractometer plot of the intact egg-shell exterior surface indicated that planes of these indices are not parallel to the shell surface, while the presence of (104), (108), and (116) peaks showed that the corresponding planes are very nearly parallel to the surface. This precluded the possibility that the *c* axis of the calcite crystals could be steeply inclined to the shell normal, as such an orientation would cause the (104) plane to be inclined at a high angle to the shell surface and could not have produced the strong (104) reflection actually observed. Such an orientation, moreover, would not have prevented the occurrence of the (110), (113), or (202) reflections which were not observed in the diffractometer experiment. The remaining range of orientations described by the reference sphere technique, however, was consistent with the diffractometer information: if the *c* axis were inclined between 12° and 45° (*i.e.* in the range 28° ± 16°) from the shell normal, the (104), (108), and (116) planes all would be approximately equally inclined at low angles to the surface of the shell and could easily have produced the corresponding reflections which were observed in the diffractometer pattern. In addition, the (110), (113), and (202) planes would in this case be nearly perpendicular to the shell surface and could not have contributed their reflections to the diffractometer trace, in agreement with observation.

It was therefore concluded that the hexagonal *c* axis (of length 17.06 A) of the calcite crystals in the outer layer of the egg shell must be inclined at 28° ± 16° from the normal to the shell surface.

It should be noted that the preparation of the photographic patterns utilized in this pole-figure technique necessitated the use of a sample considerably smaller than that employed in the diffractometer studies. As seen from Table I, the photographic patterns of the two series are not always identical for a given tilt angle. Whereas these differences seem to be indicative of an additional preferred orientation along some direction in the plane of the shell, this interpretation is not in agreement with the observation that a rotation of the larger sample in the diffractometer produced no noticeable change in the pattern recorded. The lack of complete correspondence between members of the two photographic series can be attributed to the limited number of crystallites within the small sample (a conclusion supported by the large crystallite

size found in this outer layer of the shell, described above) or by a spherulitic configuration of the crystalline phase in the tangential plane.

The authors wish to thank Dr. J. Howes of the Auburn University Poultry Science Department for bringing this problem, which is important in connection with egg-shell strength, to their attention.

A. N. J. Heyn, Professor of Physics, Auburn University, Auburn, Alabama. Present affiliation, Chairman of the Department of Biology, Louisiana State University, New Orleans. Work carried out by C. J. Cain in partial fulfillment of the requirements for the degree of Master of Science, Auburn University, Auburn, Alabama.

This work is related to a program in biological ultrastructure, supported by the National Science Foundation.

Received for publication, October 24, 1962.

REFERENCES

ABORN, R. H., and DAVIDSON, R. L., X-ray studies of particle size in silica, *J. Franklin Inst.*, 1929, **208**, 59.

CAIN, C. J., X-ray diffraction studies on the crystalline structure of the avian egg shell, Thesis, Master of Science, Auburn University, August 24, 1962.

FOULKES, R. H., PARSONS, J., and SCHUKNECHT, H. F., X-ray diffraction of otoliths and egg shells of bird and reptile, *Am. Naturalist*, 1958, **92**, 319.

HEYN, A. N. J., Electron microscope observations on the structure of calcite in the avian egg shell, *J. Appl. Physics*, 1963*a*, **33**, 2658.

HEYN, A. N. J., The crystalline structure of calcium carbonate in the avian egg shell; an electron microscope study, *J. Ultrastruct. Research*, 1963*b*, **8**, 176.

MAYNEORD, W. V., An X-ray study of the crystal structure of some biological objects, *Brit. J. Radiol.*, 1927, **22**, 19.

STEWART, G. F., The structure of the hen's egg shell, *Poultry Sc.*, 1935, **14**, 24.

YOUNG, J. D., The structure and some physical properties of the testudinian egg shell, *Proc. Zool. Soc. London*, 1951, **120**, 455.

Note Added in Proof. During the printing of this article the following excellent publications appeared on light microscopy of the avian egg shell; the findings are in agreement with those reported here:

SCHMIDT, W. J., Liegt der Eischalenkalk der Vögel als submikroskopische Kristallite vor?, *Z. Zellforsch. u. Mikroskop. Anat.*, 1962, **57**, 848.

SCHMIDT, W. J., Über die basalkalotten der Vogeleischale, *J. Ornithol.*, 1962, **103**, 28.

TEREPKA, A. R., Structure and calification in avian egg shell, and organic-inorganic interrelationships in avian egg shell, *Exp. Cell Research*, 1963, **30**, 171.